Comparison of Unconfined and Confined Micro-scale Impinging Jets

Kyo Sung Choo · Young Jik Youn · Sung Jin Kim †

Key Words : Micro-scale Impinging Jet(마이크로 스케일 충돌제트), Micro-scale Impingement Cooling(마이크로 스케일 충돌 냉각), Confined Slot jet

Abstract

In the present study, effects of degree of confinement on heat transfer characteristics of a micro-scale slot jet impinging on a heated flat plate are experimentally investigated. The effects of Reynolds numbers (Re = 1000~5000), lateral distances (x/B = 1~10), nozzle-to-plate spacings (Z/B = 1~20), and degree of confinement (B_C/B = 3, 48) on the Nusselt number are considered. The results show that the effects of the degree of confinement on the cooling performance of the micro-scale impinging slot jet are significant at lower nozzle-to-plate spacings and higher Reynolds numbers. In addition, it is shown that the cooling performance of the micro-scale unconfined slot impinging jet is 200% higher than that of the micro-scale confined slot impinging jet.

1. Introduction

An impinging jet is widely used in many engineering applications for the heating, cooling, and drying of surfaces because it has highly localized heating, cooling, and drying rates. Major industrial applications of the impinging jet include turbine blade cooling, electronic equipment cooling, metal annealing, and textile drying. For this reason, there have been many investigations on the heat transfer characteristics of macro-scale impinging jets in the past decades [1-4]. Martin [1] presented a comprehensive review on impinging jets and provided extensive heat transfer correlations for a single jet and jet arrays.

Recently there has been an interest in applying the impinging jet to small-scale devices as electronic components become smaller and smaller. Shen and Gau [5] conducted an experiment for a micro-scale impinging jet with an unconfined slot width of 200 μm. However, the confined impinging jet is more inevitable than the unconfined impinging jet in many applications due to spatial claims or installation limitations. Despite the importance of considering the confinement in the design of the micro-scale impingement cooling system, there has been no study of the micro-scale confined impinging jet.

The purpose of the present study is to find the effects of the degree of confinement on the heat transfer characteristics of the micro-scale slot impinging jet. The experimental parameters include Reynolds numbers (Re = 1000~5000), lateral distances from the stagnation point (x/B = 0~10), nozzle-to-plate spacings (Z/B = 1~20), and degree of confinement (B_C/B = 3, 48) on the Nusselt number are considered.

† Korea Advanced Institute of Science and Technology
E-mail : sungjinkim@kaist.ac.kr
TEL : (042)869-3043 FAX : (042)869-8207

2. Experimental apparatus and procedures

A schematic diagram of the experimental apparatus is shown in Figure 1. The entire apparatus was fixed on an optical table to isolate the vibration. Compressed air passed through a flexible tube and a long straight SUS pipe before entering a micro-scale unconfined slot nozzle. The airflow was supplied by a high-pressure tank to furnish a very clean and steady flow. The flow was then regulated and controlled by a mass flow controller (Brooks 5850E) with a measurement accuracy of ±1%. The flow velocity was determined from the mass flow rate near the exit of the nozzle. The micro-nozzle was fixed on an X-Y-Z stage made by Thorlabs, Inc. Thus, the nozzle could be moved either parallel or perpendicular to the direction of the jet.

As shown in Figure 2, the heated flat plate is composed of a balsawood flat plate, a gold-coated film heater with a polymer substrate, E-type thermocouples and two copper electrodes. The 30 x 30 mm² balsawood plate is 0.8 mm thick and has a low thermal conductivity. A Styrofoam insulation plate of 60 x 60 x 40 mm³ was placed behind the balsawood plate to minimize heat losses. The transparent vacuum-deposited gold-coated film heater, 20 mm long by 10 mm wide, has a polymer substrate thickness of 50 μm and a coated gold thickness of 10 nm. The film heater was glued to the balsawood plate. Two copper-foil strip electrodes with a thickness of 0.1 mm were attached to the film heater. Then, silver paint was applied to establish a good electrical contact between the electrode and the upper surface of the film

heater. The electrodes were connected to a DC power supply (HP6555A) in series with a shunt, rated 50 mV and 5 A, allowing adjustable DC voltage to the electrodes. With DC electric current applied to the film heater, a nearly uniform wall heat flux boundary condition was established. In order to measure the surface temperature, an E-type thermocouple of diameter 80 μm was installed between the balsawood plate and the film heater. The temperature distribution on the heated surface was measured using the thermocouple by controlling the X-Y-Z stage. E-type thermocouples were also attached on each face of the Styrofoam to obtain the heat losses. Lastly, the thermocouples were connected to the HP3852A data acquisition system. In order to find the effects of the degree of confinement on the heat transfer characteristics of the micro-scale slot impinging jet, four different nozzles were tested in the experiment as shown in Figure 3. The nozzles have a cross-section area of 0.25 mm x 10mm with an aspect ratio of 48. The nozzles inner width (B) is maintained constant at 0.25 mm and the outer width (B_c) is 0.75mm and 12mm respectively.

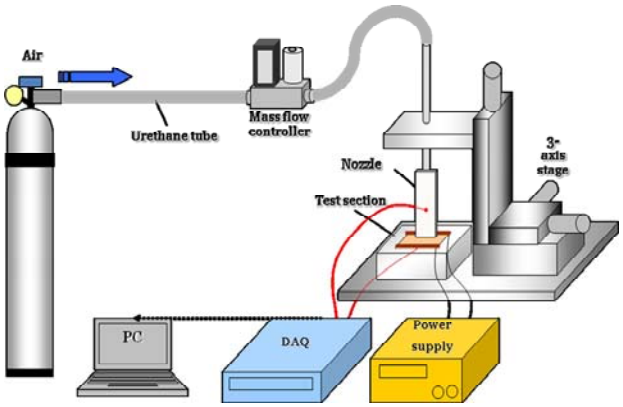

Fig. 1 Schematic of experimental set-up

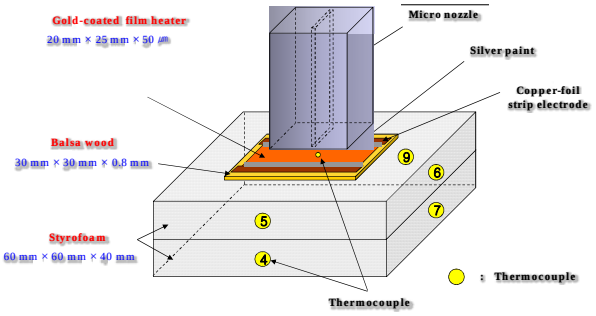

Fig. 2 Test section configuration

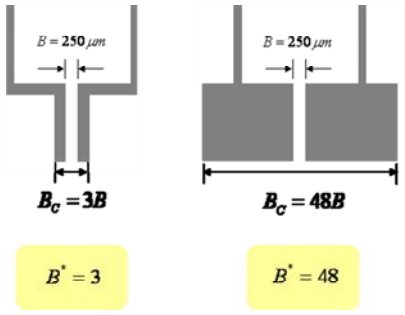

Fig. 3 Experimental parameters and nozzle geometry.

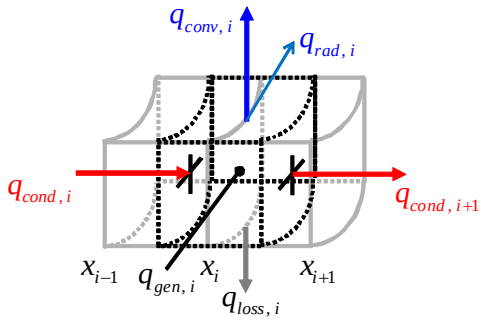

Fig. 4 Segment of annular control volume of a heater.

3. Data analysis and reduction

The local convective heat transfer coefficient and corresponding Nusselt number for the i^{th} control volume were calculated using the following equation:

$$h_i = \frac{q_{conv,i}}{A_i\left(T_i - T_{in}\right)}, \quad Nu_i = \frac{h_i B}{k_f} \tag{1}$$

For a given control volume, illustrated in Figure 4, the convective heat q_{conv} from the upper control volume surface was calculated using the following equation:

$$\begin{aligned} q_{conv,i} &= q_{gen,i} + q_{cond,i} - q_{rad,i} - q_{loss,i} \\ &= VI + (wt)k\left(\left.\frac{dT}{dx}\right|_{i+1} - \left.\frac{dT}{dx}\right|_{i}\right) \\ &\quad - \varepsilon_i \sigma A_i\left(T_i^4 - T_\infty^4\right) - \overline{h}_S A_S\left(T_S - T_\infty\right) \end{aligned} \tag{2}$$

In the analysis, the radiation heat q_{rad} was calculated from the Stefan-Boltzmann equation and the result is less than 0.5% of the total imposed heat. The heat losses q_{loss} were obtained by measuring the temperature and applying the average Nusselt number correlation for free convection on each face of the Styrofoam [6]. The maximum heat losses from the heated surface to the ambient temperature are estimated to be about 5% of the total imposed heat.

The lateral conduction q_{cond} was calculated by

solving the one-dimensional energy equation along the lateral direction of the plate. A higher lateral conduction distorts the measurement accuracy of the surface temperature. Patil and Narayanan [7] indicated that the lateral conduction along a heated plate made a significant contribution to the convective heat for the micro-scale circular impinging jet. The lateral conduction has the same order of magnitude as the amount of heat supply to an Inconel foil substrate with a thermal conductivity of k = 15 W/mK and a thickness of t = 25.4 μm. In present study, a polymer substrate with a thermal conductivity of k = 0.4 W/mK and a thickness of t = 50 μm was used in order to reduce lateral conduction. The thermal conductivity of the polymer substrate used in this study is twenty times lower than that of the Inconel foil substrate. The lateral conduction in the present study is less than 5% of the total imposed heat.

4. Results and discussion

4.1 Influence of lateral distance

In order to find the effects of the degree of confinement on the heat transfer characteristics of the micro-scale slot impinging jet, the effect of lateral variation of the local Nusselt number was considered. Figure 5 illustrates the lateral variation of the local Nusselt number at Z/B = 3 and Reynolds numbers of Re = 1000. The local Nusselt number distribution has a bell shape. The local Nusselt number decreases with increasing lateral distance.

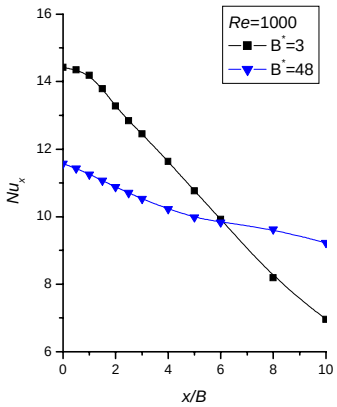

Fig. 5 Lateral variation of the local Nusselt number at Z/B = 3.

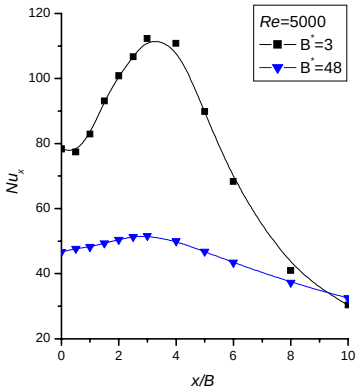

Fig. 6 Lateral variation of the local Nusselt number at Z/B = 3.

At a high Reynolds number of Re = 5000, as shown in Figure 6, the local Nusselt number exhibits a secondary peak at around x/B = 3.5. The local Nusselt number increases with increasing lateral distance from the stagnation point to the secondary peak and decreases monotonically beyond the secondary peak. The lateral variation of the local Nusselt number has a maximum value at the secondary peak location. This phenomenon is observed for the macro-scale circular impinging jet at higher Reynolds numbers and a lower nozzle-to-plate spacing [8]. The transition from laminar to turbulent flows contributes the enhancement of heat transfer in the shear layer, and this transition causes the secondary peak. The local Nusselt number increases with decreasing the degree of confinement up to the position of x/B = 8. However, the magnitude of Nusselt numbers has same values beyond the position of x/B = 8. The effects of the degree of confinement are diminished as the lateral distance moves away from the stagnation point. As shown in Figure 5 and 6, the point of intersection is moves away from x/B = 6 to x/B = 8 with increasing Reynolds number.

4.2 Influence of nozzle-to-plate spacing

The variation of the stagnation Nusselt number for nozzle-to-plate spacing is shown in Figure 7. It can be seen from this figure that the variation of the stagnation Nusselt number (Nu_0) with respect to the nozzle-to-plate spacing (Z/B) exhibits a complex nature that may not be monotonic depending on the Reynolds number. At Reynolds numbers of Re = 1000, there are humps, as can be seen in Figure 7. A similar non-monotonic behavior was also observed for the macro-scale slot impinging jets investigated by Gardon and Akfirat [3] and Sparrow and Wong [2]. The stagnation Nusselt number of B^* = 3 is 1.45 times higher than that of B^* = 48 at Reynolds number of Re = 1000 and Z/B = 1.

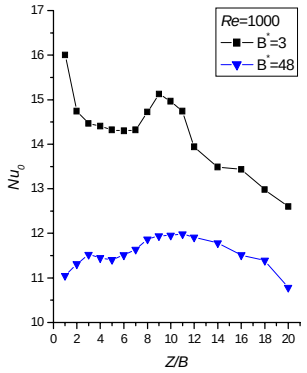

Fig. 7 Variation of the stagnation Nusselt number with nozzle-to-plate spacing at *Re* = 1000.

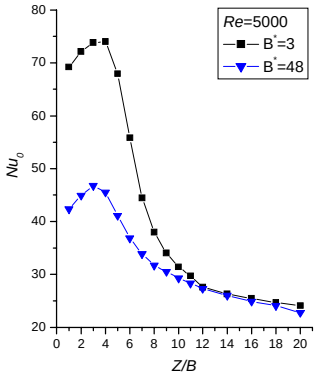

Fig. 8 Variation of the stagnation Nusselt number with nozzle-to-plate spacing at *Re* = 5000.

At a high Reynolds number of *Re* = 5000, a maximum stagnation Nusselt number occurs at around *Z/B* = 4, as can be seen in Figure 8. The stagnation Nusselt number increases as the nozzle-to-plate spacing increases from the stagnation point to the location of the maximum stagnation Nusselt number. It decreases beyond the location of the maximum stagnation Nusselt number. This trend is consistent with the results of Martin [1], Gardon and Akfirat [3], and Zhou and Lee [4]. It is well known that the variation of the stagnation Nusselt number according to nozzle-to-plate spacing is mainly affected by the potential core [3, 4]. The stagnation Nusselt number increases with decreasing the degree of confinement up to the position of *Z/B* = 12. However, the stagnation Nusselt numbers have same values beyond the position of *Z/B* = 12. The effects of the degree of confinement are diminished as the nozzle-to-plate spacing moves away from the impinging plate.

5. Conclusion

In the present study, effects of degree of confinement on heat transfer characteristics of a micro-scale slot jet impinging on a heated flat plate are experimentally investigated. The effects of Reynolds numbers (*Re* = 1000~5000), lateral distances (*x/B* = 1~10), nozzle-to-plate spacings (*Z/B* = 1~20), and degree of confinement (B_C/B = 3, 48) on the Nusselt number are considered. The results show that the effects of the degree of confinement on the cooling performance of the micro-scale impinging slot jet are significant at lower nozzle-to-plate spacings and higher Reynolds numbers. In addition, it is shown that the cooling performance of the micro-scale unconfined slot impinging jet is 200% higher than that of the micro-scale confined slot impinging jet.

Acknowledgement

This work was supported by the Korea Science and Engineering Foundation (KOSEF) through the National Research Lab. Program funded by the Ministry of Science and Technology (No. M10600000224O6J000022410).

Reference

(1) H. Martin, 1977, “Heat and mass transfer between impinging gas jets and solid surface,” *Adv. Heat Transfer* Vol. 13, pp. 1-60.

(2) E.M. Sparrow, T.C. Wong, 1975, “Impingement transfer coefficients due to initially laminar slot jets,” *Int. J. Heat Mass Transfer* Vol. 18, pp. 597-605.

(3) R. Gardon and J.C. Akfirat, 1966, “Heat transfer characteristics of impinging two dimensional air jets,” *J. Heat Transfer*, Vol. 88, pp. 101-108.

(4) D.W. Zhou and S.J. Lee, 2007, “Forced convective heat transfer with impinging rectangular jets,” *Int. J. Heat Mass Transfer*, Vol. 50, pp. 1916-1926.

(5) C.H. Shen and Gau, 2004, “Heat exchanger fabrication with arrays of sensors and heaters with its micro-scale impingement cooling process analysis and measurements,” *Sensors and Actuators A* Vol. 114, pp. 154-162.

(6) F.P. Incropera and D.P. DeWitt, 2002, “Introduction to heat transfer,” John Wiley & Sons, Inc., New York.

(7) V.A. Patil and V. Narayanan, 2005, “Spatially resolved heat transfer rates in an impinging circular microscale jet,” *Microscale Thermophys. Eng.*, Vol. 9 , pp. 183-197.

(8) H. M. Hofmann, M. Kind, H. Martin, 2007, “Measurements on steady state heat transfer and flow structure and new correlations for heat and mass transfer in submerged impinging jets,” *Int. J. Heat Mass Transfer* Vol. 50, pp. 3957-3965.